JMEPEG (1999) 8:245-251

Fatigue Crack Propagation Behavior in Dual-Phase Steel

M. Sarwar and R. Priestner

(Submitted 27 January 1998; in revised form 15 September 1998)

The fatigue crack propagation in dual-phase steel was studied with the objective of developing ferritic-martensitic microstructures via intercritical annealing and thermomechanical processing. It was found that the changes in fatigue crack propagation rates and in the threshold stress intensity range, ΔK_{th}, resulting from microstructural variations, were directly related to tensile strength in the same manner that was observed in other types of structural steels. It was also observed that the relationship between tensile strength and fatigue crack propagation in intercritically annealed and thermomechanically processed dual-phase steel was much the same as for conventional steels of similar strength level.

Keywords crack growth, dual-phase steel, fatigue, martensite

1. Introduction

The fatigue crack propagation rate has been shown in various studies to depend on the stress intensity parameter, mean stress, load ratio, and environment. Many of these measurements were made in an intermediate crack growth region. However, more recent interest has been directed to crack propagation at very low stress intensities and to the determination of thresholds for fatigue crack growth.

The most dramatic results on fatigue crack growth (FCG) resistance of dual-phase steels were reported by Suzuki and McEvily (Ref 1) and Minakawa et al. (Ref 2), who developed two different microstructures in an AISI 1018 steel. One steel was continuous ferrite matrix encapsulated islands of martensite (FEM), and the other was a continuous martensite constituent with encapsulated islands of ferrite (MEF). It was reported that the FEM microstructure had a lower threshold ΔK value and higher fatigue crack growth rate than the MEF microstructure. Wasynczuk et al. (Ref 3) and Suresh and Richie (Ref 4) showed that the threshold values were unaffected by changing the volume fraction of martensite from 35 to 48% and 32 to 58%, respectively. Geric and Drobnjak (Ref 5) also reported that the fatigue threshold value of ΔK was unaffected by volume fraction of martensite. Obviously, the influence of volume fraction of martensite on the (near threshold) fatigue crack propagation has not been fully investigated, and no quantitative relationship to microstructural parameters has been reported so far.

In this work, the influence of dual-phase microstructures with different morphologies and volume fractions of martensite on near threshold fatigue crack growth were studied.

2. Experimental Work

The chemical composition (wt%) of steel used was:

Element	Chemical composition, wt%
Fe	bal
C	0.16
Mn	1.03
Cr	0.14
Si	0.24
Mo	0.04
Ni	0.15
Cu	0.20

Each specimen is coded according to the treatment it was given (i.e., 50BQ780). The left number represents the amount of rolling deformation, the center letters represent the cooling medium used (BQ, ice-brine quenched; HWQ, hot water quenched; and OQ, oil quenched), and the right number represents the intercritical annealing temperature.

2.1 Heat Treatment for Mechanical Testing

In order to study fatigue crack propagation, blanks 6 mm thick, 180 by 45 mm in area (for 0% reduction), and 12 mm thick, 130 by 45 mm in area (for 50% reduction), were obtained from the original plates. These blanks were divided into four groups for intercritical heat treatment (ICHT) and thermomechanical processing (TMP) to obtain different amounts of martensite and different microstructural morphologies. A swift semiautomatic point counter was used to determine the volume fractions of various constituents present. For each specimen, 1000 to 1500 points were counted at a magnification of 400 and 1000×.

Group I. The blanks, 6 mm thick, were intercritically annealed at 780 °C for 20 min and quenched in ice brine or hot water (at 86 °C) to produce 55 and 30% martensite, respectively.

Group II. Blanks 12 mm initial thickness were heat treated at 780 °C for 20 min, rolled to a 50% reduction, and quenched in ice brine or oil to produce the same amounts of martensite mentioned in group I.

Group III. Blanks, as in group I, were intercritically annealed at 740 °C for 20 min to produce 30% austenite and then quenched in ice brine.

Group IV. Blanks with the same initial thickness as group II were heat treated at 740 °C for 20 min, rolled to a 50% reduction, and then quenched in ice brine.

M. Sarwar, PAEC, Dera Ghazi Khan, Pakistan; and **R. Priestner,** Manchester Materials Science Center, Manchester, England.

2.2 *Fatigue Testing*

Threshold Stress Intensity Tests. The single edge-notched tension type of specimens were machined from the processed blanks for fatigue crack growth tests. Figure 1 (Ref 6) shows the dimensions. The edge notch was spark machined. Both surfaces of each specimen were prepared by coarse grinding on silicon carbide paper followed by polishing with 6 and 1 μm diamond paste.

The fatigue tests were carried out using an Instron electrohydraulic testing machine (Model 1255) (Instron, Canton, MA). All tests were conducted under load control. The frequency of testing was between 5 and 30 Hz, depending upon the crack growth rate. The wave form was sinusoidal. The specimens were tested at room temperature in an ambient atmosphere. The test load was parallel to the rolling direction. Tests were conducted at load ratios, R, of 0.05, 0.3, and 0.5 (where $R = \sigma_{min}/\sigma_{max}$).

For the determination of the threshold stress intensity range, ΔK_{th}, a stepwise, ΔK decreasing method was used. The crack initially grown 1 mm from the notch tip and load was then progressively decreased by approximately 10% of the current level at each step. This procedure was followed until a stress intensity range was reached (corresponding to $da/dN = 4 \times 10^{-10}$ m/cycle), at which no detectable growth occurred. This stress intensity range was designated as the threshold level, ΔK_{th}. Once the threshold value was determined, the load was increased gradually until the termination of the test.

The crack length, a, was measured at both surfaces of the specimen, on one side by using a traveling telescope having an eyepiece with an engraved scale. A sinate lens reflex (SRL) camera was used to take photographs of the other surface of the specimen, from which crack lengths were measured.

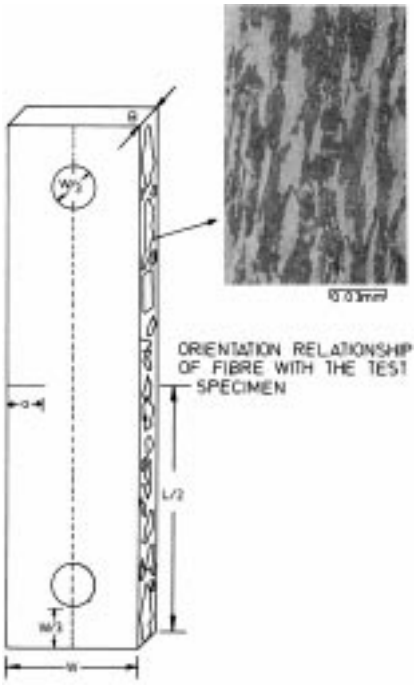

Fig. 1 An illustration of orientation relationship of fibers with the test specimen

The stress intensity factor range, ΔK, was calculated according to the following relationship (Ref 7):

$$\Delta K = \Delta P/BM \sqrt{\pi\alpha}\ F(\alpha)$$

where $\alpha = a/W$, and:

$$F(\alpha) = 1.212 - 0.231\alpha + 10.55\alpha^2 - 21.72\alpha^3 + 30.39\alpha^4$$

where ΔP = applied load range = $P_{max} - P_{min}$, B is thickness of the specimen, W is width of the specimen, and a is crack length.

3. Results and Discussion

3.1 *Fatigue Crack Propagation*

The intercritical heat treatments and thermomechanical treatments were selected to provide comparisons between high and low martensite contents, between fibrous and nonfibrous morphologies of martensite, and between dissimilar contents of epitaxial ferrite. Figure 2 indicates the microstructure of dual-phase steel after intercritical annealing at 780 °C and quenching in hot water. It should also be kept in mind that different processing steps required to provide these comparisons also varied the apparent ferrite grain size, the mean linear free path in ferrite between martensite particles, and the substructure in the ferrite.

3.2 *Effect of Martensite Content on ΔK (Threshold)*

Specimen 0BQ780 and 0BQ740 contained 55 and 31% martensite, respectively. Both specimens were brine quenched, so the amount of epitaxial ferrite was virtually zero in each. Table 1 indicates the threshold stress-intensity factor (ΔK_{th}) was almost the same, over the range of R from 0.05 to 0.5, for both volume fractions of martensite. Direct comparison of the da/dN

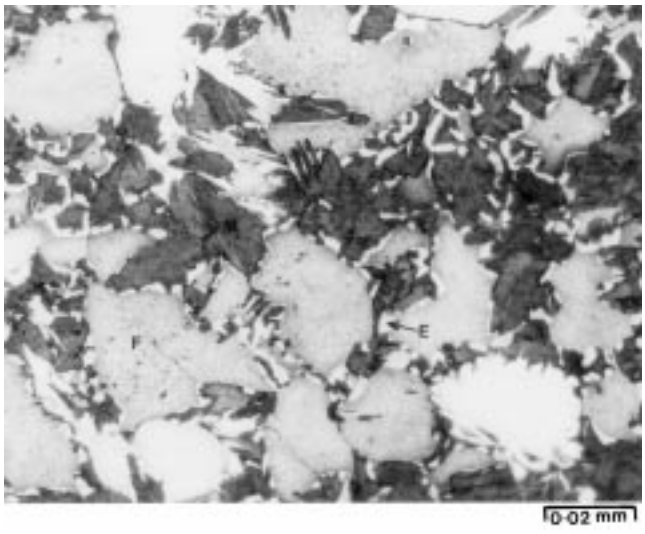

Fig. 2 Microstructure of dual-phase steel after intercritical annealing at 780 °C and quenching in hot water. M, martensite; F, ferrite; and E, epitaxial ferrite

versus ΔK data at $R = 0.05$ (Fig. 3) and 0.5 shows that at both values of R, within experimental error, martensite content had no effect on crack growth rate within the range of ΔK studied.

The effect of martensite content in the TMP material was also negligible at high R values. However, at $R = 0.05$, crack growth rates were significantly higher in the specimen with the lower martensite content. Direct comparison of the data in Fig. 4 shows that the curve of log (da/dN) versus log (ΔK) for lower martensite content is parallel to that for the higher martensite constant at all crack growth rates and is shifted along the log ΔK axis toward lower ΔK. That is, the threshold ΔK value increased with the increase of the volume fraction of martensite.

Wasynczuk et al. (Ref 3) investigated dual-phase steel in which a "lath" morphology of martensite was generated by intercritical annealing of an initial martensitic microstructure at two different temperatures to obtain two volume fractions of martensite. The "lath" morphology arose because the austenite present at the intercritical annealing temperature grew between the original martensite laths; it was therefore unoriented. They reported that the threshold ΔK value remained constant with the variation of volume fraction of martensite.

From the Wasynczuk work (Ref 3), it appears that increasing the aspect ratio of martensite particles in dual-phase steel, but leaving them randomly oriented, did not result in ΔK threshold becoming sensitive to martensite content. In the present work, in which the high-aspect ratio martensite particles were oriented parallel to the stress axis, TMP did cause ΔK threshold to depend on martensite content, but only at the lowest R value.

3.3 Effect of Thermomechanical Processing

Specimen 0BQ780 and 50BQ780 contained approximately the same volume fraction of martensite. Both were brine quenched so the amount of epitaxial ferrite was virtually zero in each. Table 1 indicates that ΔK_{th} was higher for rolled material than for not-rolled material at $R = 0.05$, but was almost the same at a high value of R. Figure 5 shows the direct comparison of the da/dN versus ΔK data at $R = 0.05$.

Chen et al. (Ref 8) studied a 0.07% C, 1.46% Si, and 0.7 Mn steel containing different dual-phase microstructures produced by heat treatment, such that the volume fraction of the martensite was constant at 12%. They reported that the ΔK_{th} value at $R = 0$ for material containing "lath" martensite before intercritical annealing was only slightly higher than for material containing ferrite/pearlite before intercritical annealing. The initial structure of lath martensite was fibrous martensite, but unoriented in the dual-phase microstructure. The present result is that fibering of martensite parallel to the stress axis by thermomechanical processing raised ΔK_{th}, but only slightly and only at low R value. It would appear that the effect of TMP was

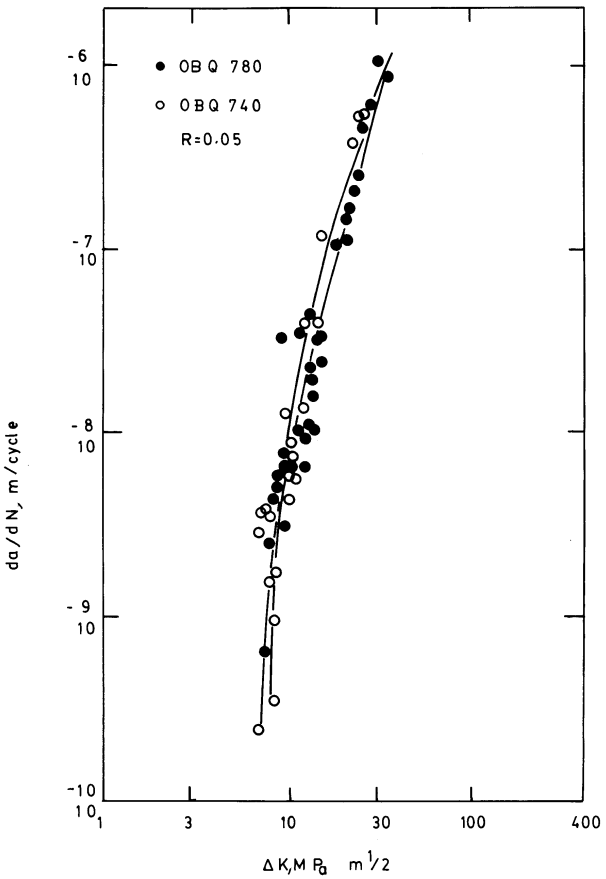

Fig. 3 Fatigue crack propagation rates (da/dN) as a function of stress intensity range (ΔK) at $R = 0.05$ for specimens 0BQ780 and 0BQ740

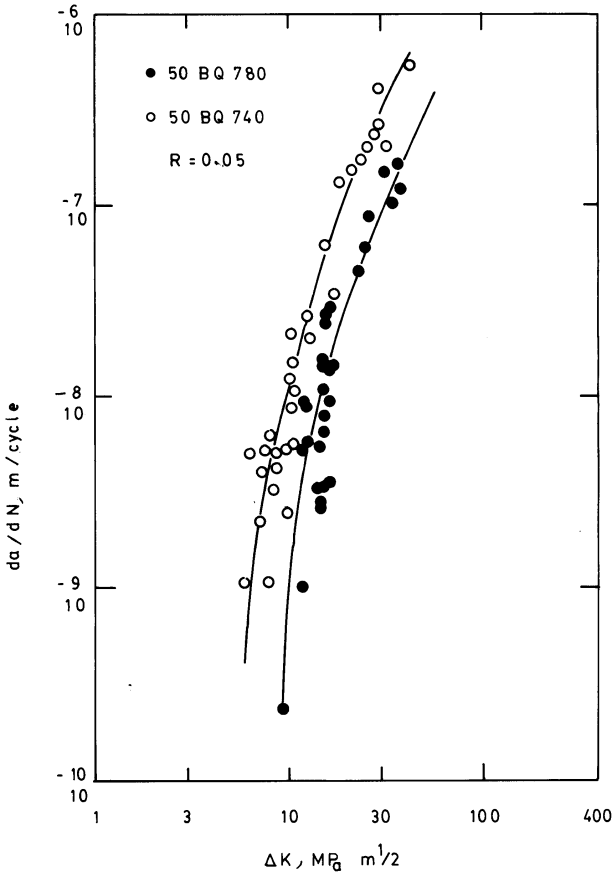

Fig. 4 Fatigue crack propagation rates (da/dN) as a function of stress intensity range (ΔK) at $R = 0.05$ for specimens 50BQ780 and 50BQ740

not related particularly to the alignment of martensite fibers, but simply to the fact that the martensite was fibrous. This effect on fibrosity was approximately 50% martensite and was not maintained at approximately 30% martensite. Specimens 50OQ780 and 0HWQ780 contained 32 and 27% volume fraction of martensite, respectively, and each had approximately 20% volume fraction of epitaxial ferrite. Figure 6 shows the comparison of da/dN versus ΔK data at $R = 0.05$. Figure 7 shows that data for specimen 0BQ740 and 50BQ780 having 30% volume fraction of martensite. Both of these specimens

Table 1 Fatigue crack propagation results

Specimen code	Volume fraction of martensite, %	Stress ratio, R	ΔK_{th} MPa m$^{1/2}$ at 4×10^{-10} m/cycle	ΔK_{th} MPa m$^{1/2}$ at 10^{-9} m/cycle
0BQ780	55	0.05	7.5	7.6
		0.5	4.0	4.8
50BQ780	48.9	0.05	9.7	10.0
		0.3	6.0	6.8
		0.5	3.8	4.0
0HWQ780	27	0.05	10.8	11.0
		0.3	8.5	9.0
		0.5	7.0	7.6
50OQ780	32	0.05	8.5	8.5
		0.3	7.2	7.7
		0.5	5.6	5.9
0BQ740	30.7	0.05	7.9	8.5
		0.3	6.5	6.5
		0.5	4.6	5.3
50BQ740	29.4	0.05	6.0	6.5
		0.3	6.5	6.6
		0.5	5.8	5.8

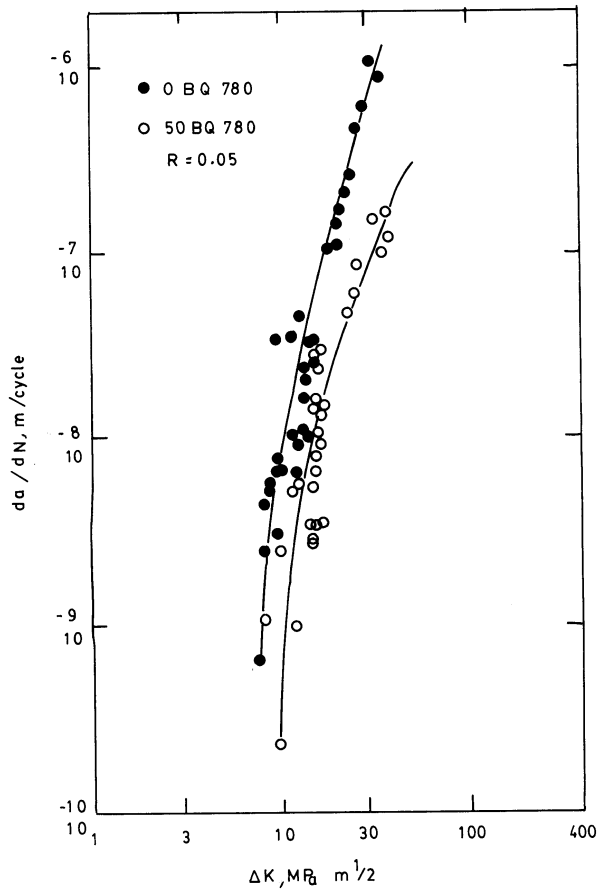

Fig. 5 Fatigue crack propagation rates (da/dN) as a function of stress intensity range (ΔK) at $R = 0.05$ for specimens 0BQ780 and 50BQ780

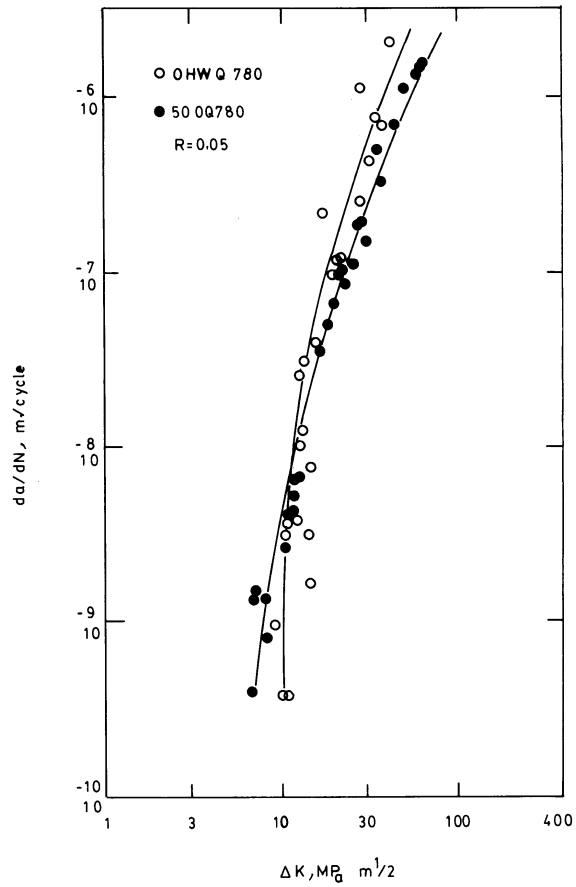

Fig. 6 Fatigue crack propagation rates (da/dN) as a function of stress intensity range (ΔK) at $R = 0.05$ for specimens 50OQ780 and 0HWQ780

were brine quenched, so the amount of epitaxial ferrite was virtually zero. It can be seen from these figures that thermomechanical processing reduced ΔK_{th} relative to intercritical heat treatment at approximately 30% volume fraction of martensite. It is also noticeable that the nonfibrous morphology led to lower crack growth rates near the threshold level, but led to higher growth rates for values of da/dN above 10^{-8} m/cycle.

3.4 Effect of Epitaxial Ferrite Content on ΔK (Threshold)

Specimen 0BQ740 and 0HWQ780 contained approximately similar contents of martensite but dissimilar contents of epitaxial ferrite. Figure 8 directly compares the da/dN versus ΔK data at $R = 0.05$. The curve for lower epitaxial ferrite content is parallel to that for higher epitaxial content at all crack growth rates and is moved along the log ΔK axis toward lower ΔK. This figure suggests that the presence of epitaxial ferrite increased the ΔK threshold. Similar behavior was also observed for rolled materials, as shown in Fig. 9.

Figure 10 shows ΔK_{th} depended on the volume fraction of martensite at the load ratio of 0.05. Data from Ref 2, 3, and 8 to 10 are also plotted with the present results for comparison. The general trend of the data suggests that ΔK_{th} decreases with an increase of the volume fraction of martensite.

In view of the present results, it may be that the general trend is superficial. As described earlier, direct comparison of crack growth data for specimens containing different martensite contents but the same epitaxial ferrite content revealed no significant influence of martensite contents. However, epitaxial ferrite appears to raise ΔK_{th}. Thus a specimen containing 30% martensite plus 20% epitaxial ferrite should have a higher ΔK_{th} than one containing 50% martensite and no epitaxial ferrite. It follows that when the data are plotted versus martensite content, as in Fig. 10, ΔK_{th} will appear to decrease with increasing martensite.

It is not known whether the data in literature can be explained in the same way because the microstructures were not categorized as carefully as in this study. However, very fast quenching is needed to avoid epitaxial ferrite completely, and it is possible that in general for data reported previously, lower martensite contents were accompanied by higher contents of epitaxial ferrite.

3.5 Effect of Strength on ΔK_{th}

The variation of threshold value with 0.2% proof stress and ultimate tensile strength, plotted in Fig. 11 and 12, respectively, indicate a general trend of an inverse dependence of ΔK_{th} on material strength. The present results are in agreement with previous data, also plotted in Fig. 11 and 12.

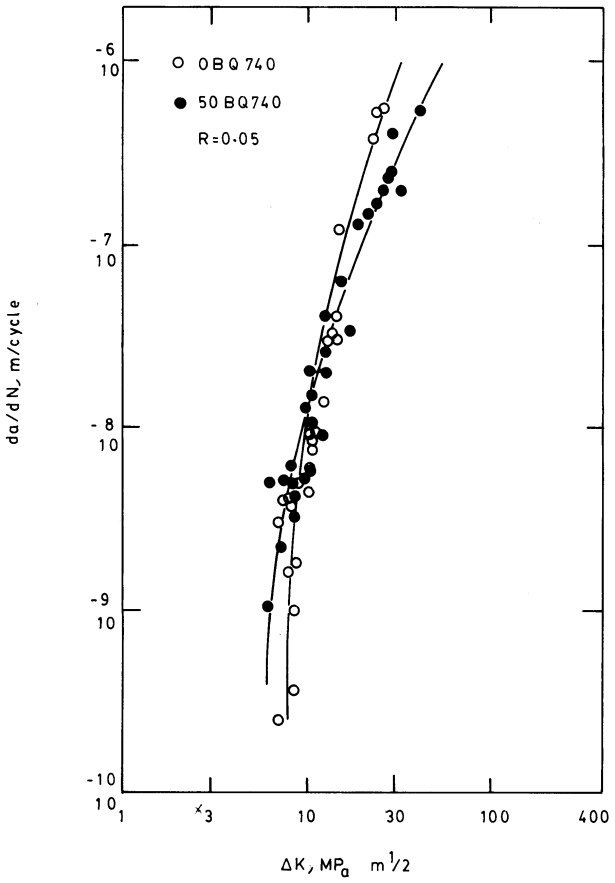

Fig. 7 Fatigue crack propagation rates (da/dN) as a function of stress intensity range (ΔK) at $R = 0.05$ for specimens 0BQ740 and 50BQ740

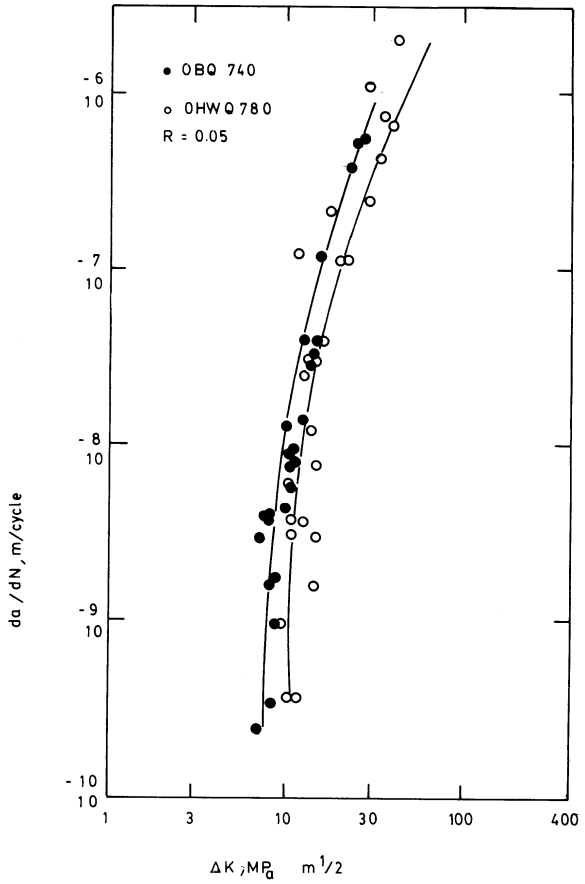

Fig. 8 Fatigue crack propagation rates (da/dN) as a function of stress intensity range (ΔK) at $R = 0.05$ for specimens 0BQ740 and 0HWQ780

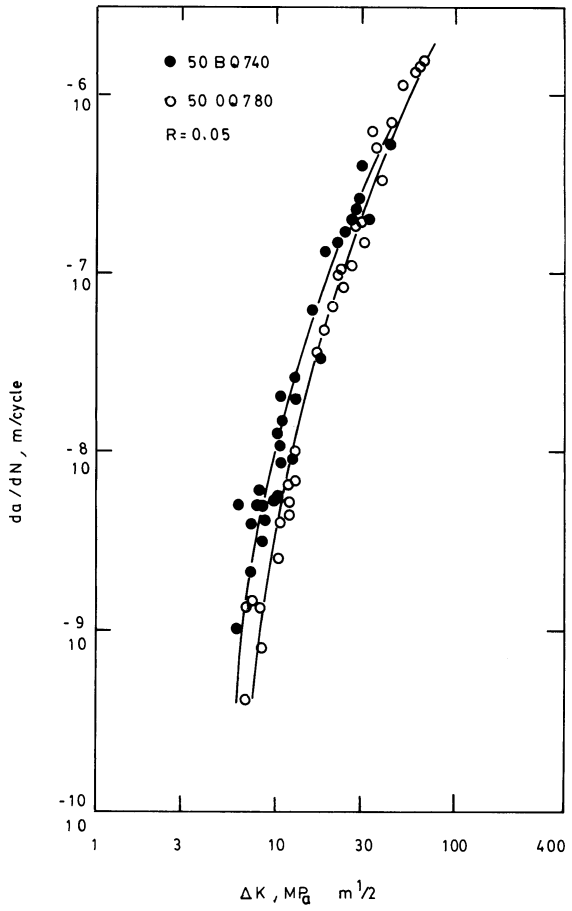

Fig. 9 Fatigue crack propagation rates (*da*/*dN*) as a function of stress intensity range (Δ*K*) at *R* = 0.05 for specimens 50BQ740 and 50BQ780

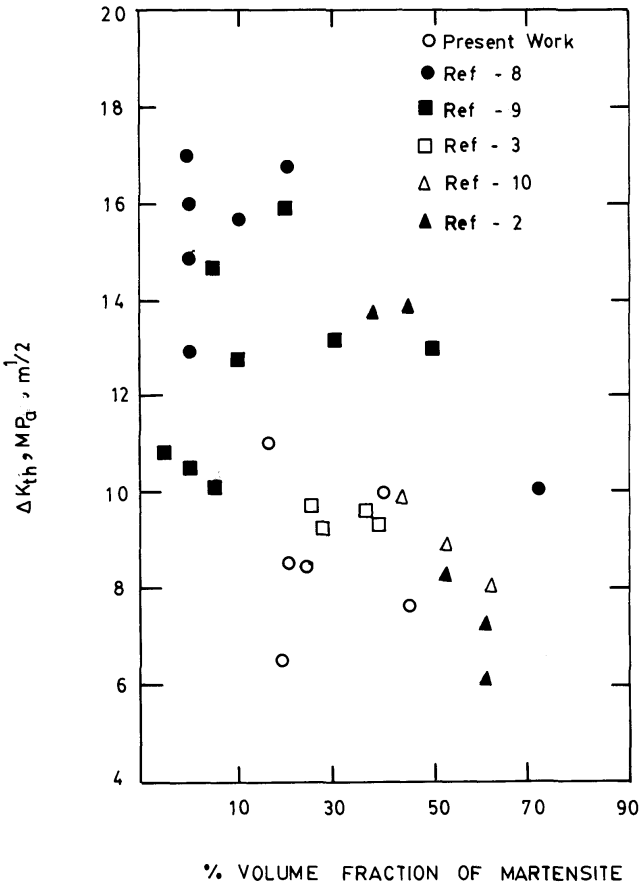

Fig. 10 Variation of ΔK_{th} value with the volume fraction of martensite, $R = 0.05$

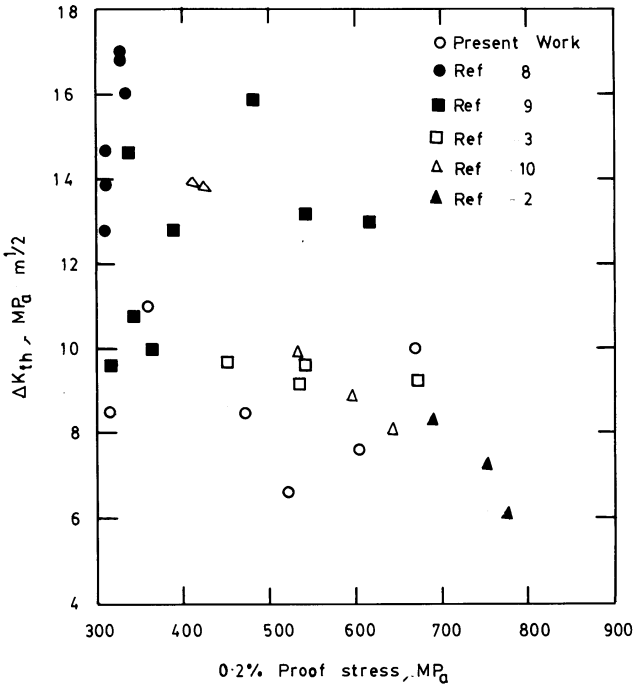

Fig. 11 Variation of ΔK_{th} value with proof stress

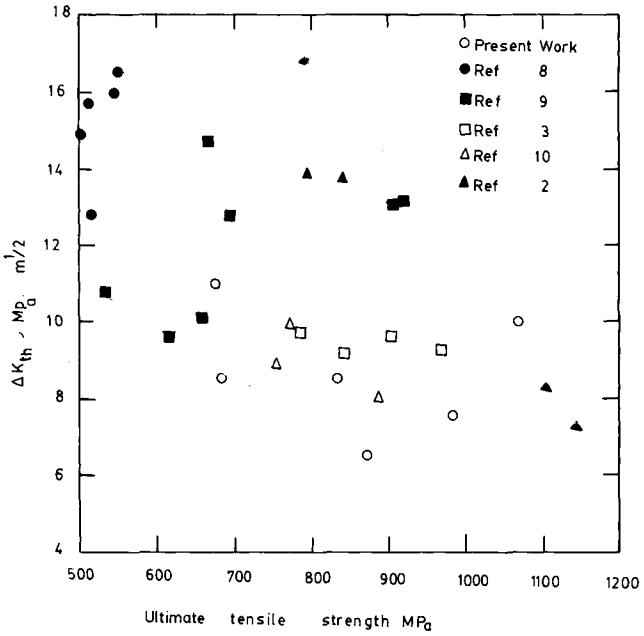

Fig. 12 Variation of ΔK_{th} value with ultimate tensile strength

4. Conclusions

- High volume fraction of martensite increased the ΔK_{th} only for rolled material when the epitaxial ferrite was virtually zero and only at a low value of R. The ΔK_{th} value remained constant with martensite content for not-rolled material. At lower volume fraction of martensite, thermomechanical processing reduced ΔK_{th}, the relative intercritical heat treatment, at approximately 30% martensite.
- The presence of epitaxial ferrite increased the ΔK threshold for both rolled and not-rolled material. Thus a material containing 30% martensite plus 20% epitaxial ferrite had a higher ΔK_{th} value than one containing 30% martensite and no epitaxial ferrite.
- An inverse dependence of ΔK_{th} on strength was observed.
- Generally, the fatigue threshold ΔK values were of similar magnitude as for other structural steels of similar strength.

References

1. H. Suzuki and A.J. McEvily, *Metall. Trans. A*, Vol 10, 1979, p 475
2. K. Minakawa, Y. Matuso, and A.J. McEvily, *Metall. Trans. A*,Vol 13, 1982, p 439
3. J.A. Wasynczuk, R.O. Richie, and G. Thomas, *Mater. Sci. Eng.*, Vol 62, 1984, p 79-93
4. D.S. Suresh and R.O. Richie, *Metall. Trans. A*, Vol 115, 1984, p 1193-1207
5. K. Geric and D. Drobnjak, *Fracture Control of Engineering Structure ECF*, Vol 5, Lisbon, 1984, p 115-123
6. *Stress Intensity Factor*, Vol 1, The Society of Materials Science, Japan, 1987, p 9
7. W.F. Brown, Jr. and J.E. Srawley, ASTM STP 410, 1966, p 12
8. D.L. Chen, Z.G. Wang, X.X. Jaing, S.H. Ai, and C.H. Shih, *Scr. Metall.*, Vol 21, 1987, p 1663-1667
9. K. Geric and D. Drobnjak, *Fracture Control of Engineering Structures ECF*, Vol 3, Lisbon, 1986, p 1523-1533
10. M.K. Tseng, L. Jiang, and Z.H. Lai, *Fatigue Prevention and Design*, Amsterdam, 1986, p 21-24